2−4

NUMERICAL SIMULATIONS OF THE HYPERSONIC FLOWFIELDS AROUND OREX

Masahiro NAKAO
Mitsubishi Heavy Industries, Ltd.

The hypersonic flowfields around the OREX have been simulated by the MHI hypersonic Navier-Stokes code CHRIS(Computer code for Hypersonic Reentry Information Synthesis). This code is based on the upwind, implicit, finite-difference method using Roe's Riemann solver with MUSCL(Monotonic Upstream Schemes for Conservation Laws) type higher-order accurate formulation of the convective terms. The real gas effects are taken into consideration using a VEG(Variable Equivalent Gamma) method with simplified curve fit of equilibrium air properties. Computations for the OREX are done under the assumption of equilibrium gas and perfect gas. Comparisons between the results obtained for real gas and perfect gas calculations are discussed.

1. INTRODUCTION

Recent progress of computing power has enabled us to simulate complex and high speed flowfields numerically around complex configurations of aircraft. The flowfields around a reentry vehicles are complex and provide one of the most challenging problems in the application of the computational fluid dynamics. One of the problems of the development of the hypersonic CFD code is the lack of the test data for code validation. Because existing wind tunnel facilities may not realize such a high stagnation enthalpy flow.

The OREX(Orbital Re-Entry Experiment) flight test was done in 1994. The one of objectives of the test is to get hypersonic flow data for CFD code validation. The heat transfer, wall pressure, and electron density data were acquired in the flight tests. In 1995, the high enthalpy workshop was held in NAL(National Aerospace Laboratory) and simulation of the flowfield around OREX is included as one of the problems.

In this paper, the flowfield around the OREX was simulated using our hypersonic real gas Navier-Stokes code. Computations were done under the assumption of an equilibrium gas and a perfect gas.

2. GOVERNING EQUATIONS

Compressible, Reynolds-averaged Navier-Stokes equations are formulated in the body fixed frame.

$$\hat{Q}_\tau + \hat{F}_\xi + \hat{G}_\eta + \hat{H}_\zeta = Re^{-1}\hat{S}_\zeta$$

where

$$\hat{Q} = \frac{1}{J}\begin{pmatrix} \rho \\ \rho u \\ \rho v \\ \rho w \\ e \end{pmatrix} \qquad \hat{F} = \frac{1}{J}\begin{pmatrix} \rho U \\ \rho uU + \xi_x P \\ \rho vU + \xi_y P \\ \rho wU + \xi_z P \\ (e+P)U - \xi_t P \end{pmatrix}$$

$$\hat{G} = \frac{1}{J}\begin{pmatrix} \rho V \\ \rho uV + \eta_x P \\ \rho vV + \eta_y P \\ \rho wV + \eta_z P \\ (e+P)V - \eta_t P \end{pmatrix} \qquad \hat{H} = \frac{1}{J}\begin{pmatrix} \rho W \\ \rho uW + \zeta_x P \\ \rho vW + \zeta_y P \\ \rho wW + \zeta_z P \\ (e+P)W - \zeta_t P \end{pmatrix} \qquad (1)$$

and F, G, H are the convective flux vectors and S is the viscous flux under the thin layer approximation. J is the Jacobian of transformation and the sign^ indicates that the quantity is normalized by the Jacobian. Re is the Reynolds number. The primitive variables of Q are the density r, the three mass fluxes ru, rv, and rw in the three coordinate directions x, y, and z, respectively and the energy per unit volume e. All these variables are normalized by freestream reference values. The velocities are normalized by the free stream speed of sound. The real gas effects are taken into account using the VEG(Variable Equivalent Gamma) method [1)-2)] under the assumption of chemical and thermal equilibrium state.

In the general expression the equation of state is written in the following form:

$$P = P(\rho, \rho ei) \qquad (2)$$

where ei is specific internal energy.

Unlike the perfect-gas case, explicit expression for the pressure as a function of density and internal energy is not available. The VEG method assumes that pressure is written in the same form as perfect gas:

$$P=\rho ei(\hat{\gamma} - 1) \tag{3}$$

where gamma $\hat{\gamma}$ is not constant but the function of density and internal energy:

$$\hat{\gamma} = \hat{\gamma}(\rho, ei) \tag{4}$$

This $\hat{\gamma}$ is called equivalent gamma and is calculated from the efficient simplified curve fits developed by S. Srinivasan and C. Tannehill[3]. These curve fits have the save range of validity of NASA RGAS data, namely, temperatures up to 2500 K and densities from 10^{-7} to 10^{3} amagats (ρ/ρ_0, ρ_0 : density at reference condition at 1 atm and 273.15 K). Utilization of this equation of pressure requires no essential change in the expression of Roe's approximate Riemann solver, time integration scheme and boundary conditions for the perfect gas[4]. The gamma and pressure are calculated using the curve fits at each time step. In the real gas Navier-Stokes code, the viscosity and thermal conductivity should also be calculated in the equilibrium air. These coefficients are obtained from curve fits which have been developed again by Srinivasan et. al[5]. A modified version of LU-ADI time integration algorithm[6] is used in the present code.

3. NUMERICAL ALGORITHM

Generalized Riemann Solver

In this code generalized Roe's Riemann solver is adopted to calculate inviscid flux. The essence of Roe's scheme is the solution of local Riemann problems stemming from the consideration of piecewise uniform states between cell interfaces on an initial data line. For simplicity, non-conservative form of the equation in one-dimensional case is considered;

$$Q_t+AQ_x= 0 \tag{5}$$

where A is a (locally constant) Jacobian matrix for each pair of initial data(Q_R,Q_L), where the subscripts R and L denote the right and the left side values of the cell face. The requirements for the matrix A are described in Ref.4 and the major property is

$$\Delta F = \bar{A}\Delta Q \tag{6}$$

where $\Delta Q = Q_R - Q_L$ and $\Delta F = F_R - F_L$ is obtained using

$$\bar{A} = \bar{A}(\bar{Q}) \tag{7}$$

The above expression is known as a Roe-averaged state and was derived by Roe for a perfect gas[4]. The components of the average state of $\bar{A}(\hat{\gamma})$ are obtained as follows

$$\begin{aligned} \bar{\rho} &= \sqrt{\rho_R\rho_L} \\ \bar{u} &= \alpha u_L + (1-\alpha)u_R \\ \bar{H} &= \alpha H_L + (1-\alpha)H_R \end{aligned} \tag{8}$$

where

$$\alpha = \frac{\sqrt{\rho_L}}{(\sqrt{\rho_L}+\sqrt{\rho_R})} \tag{9}$$

An important quantity in the approximate Riemann solver is the column vector $R^{-1}\Delta Q$. Its components are the jumps in the characteristic variables. It can be expressed simply in terms of ΔP, $\Delta\rho$ and Δu as

$$R^{-1}\Delta Q = \begin{bmatrix} \Delta\rho - \Delta P/a^2 \\ \frac{1}{2}(\Delta\rho/a^2 + \Delta u/a) \\ \frac{1}{2}(\Delta\rho/a^2 - \Delta u/a) \end{bmatrix} \tag{10}$$

This has the same form as for perfect gas. In the real-gas case, pressure derivative ΔP is given as

$$\Delta P = \chi\Delta\rho + \kappa\Delta\varepsilon \tag{11}$$

where $\varepsilon = \rho e_i$ and the derivatives are denoted by

$$\chi = \left(\frac{\partial P}{\partial \rho}\right)_{\varepsilon} \quad \kappa = \left(\frac{\partial P}{\partial \varepsilon}\right)_{\rho} \tag{12}$$

Here the subscript ε (ρ) denotes the partial derivative of p with respect to ρ (ε) by holding ε (ρ) constant.

Using Eqs. (3) and (12) Eq.(11) can be expressed as follows:

$$\Delta P = \varepsilon \frac{\partial \hat{\gamma}}{\partial \rho} \Delta \rho + \left\{ \left(\hat{\gamma} - 1 \right) + \frac{\partial \hat{\gamma}}{\partial \varepsilon} \right\} \Delta \varepsilon \tag{13}$$

In Eq (13), gamma varies more slowly than the other thermodynamic variables since gamma remains between 1 and 5/3, for any combination of ρ and ε that may vary several order of magnitude . and will be very small and can be assumed to be zero. Then Eq.13 may be approximated as

$$\Delta P = \left(\hat{\gamma} - 1 \right) \Delta \varepsilon \tag{14}$$

This is the form of pressure derivative which corresponds to that of Grossman et al. [7].

Chemical Component Calculation

Chemical components of the equilibrium air are calculated by the method of Ref.9. Eleven chemically reacting species-O_2, N_2, O, NO, N, NO^+, e^-, N^+, O^+, Ar, and Ar^+ - are included. The method involves the algebraic combination of the equilibrium, elemental mass-balance, and charge-neutrality equations and solves the resulting equation by an iterative method.

Numerical Grid

Figure 1 shows the OREX configuration. This configuration simulates the nose shape of the HOPE.

In the hypersonic flow calculations, the grid adaptation technique is effective for capturing strong shock waves. In this calculation the out boundary of the grid is fitted to the bow shock by estimating pressure derivatives. Figure 2 shows the initial grid. Figure 3 shows the boundary fitted grid.

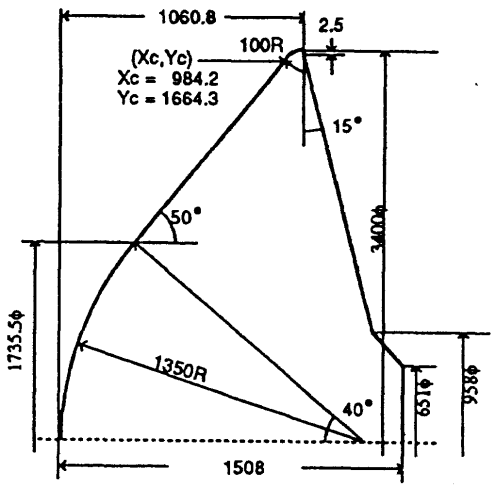

Fig. 1 OREX Configuration

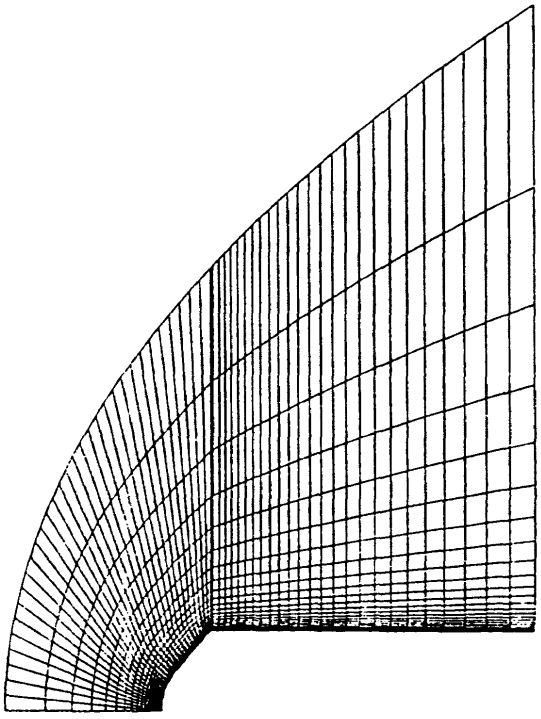

Fig. 2 Initial Grid for OREX

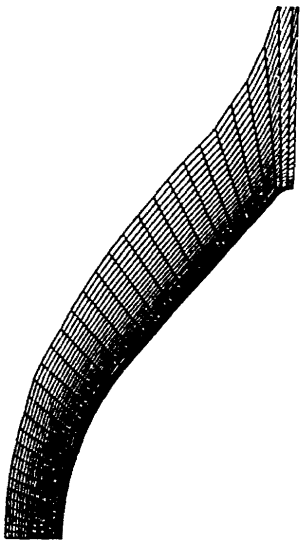

Fig. 3 (a) Grid for perfect gas case

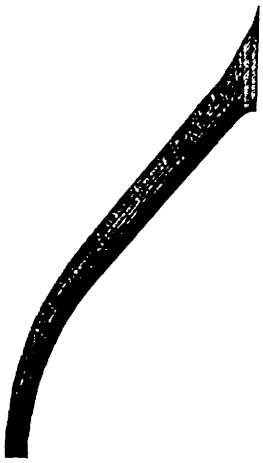

Fig. 3 (b) Grid for real gas case

4. RESULTS

The flow condition is the free stream velocity of 5562m/s, free stream temperature of 248.1 K, free stream pressure of 23.6 N/m^2 and wall temperature of 1519 K. The calculations were done under the assumption of real gas and perfect gas.

Figure 3(a) shows the numerical grid of the perfect gas case and figure 3(b) shows that of the real gas case. The number of the grid points of these two cases is the same and is 40x8x50 totaling up to about 16,000. The difference of the out boundary of the grid between the real gas and perfect gas is due to the difference of the shock stand-off distances. Figure 4 shows the comparison of computed pressure distribution between perfect gas and real gas. The shock stand-off distance of the real gas case is significantly shorter than that of the real gas case.

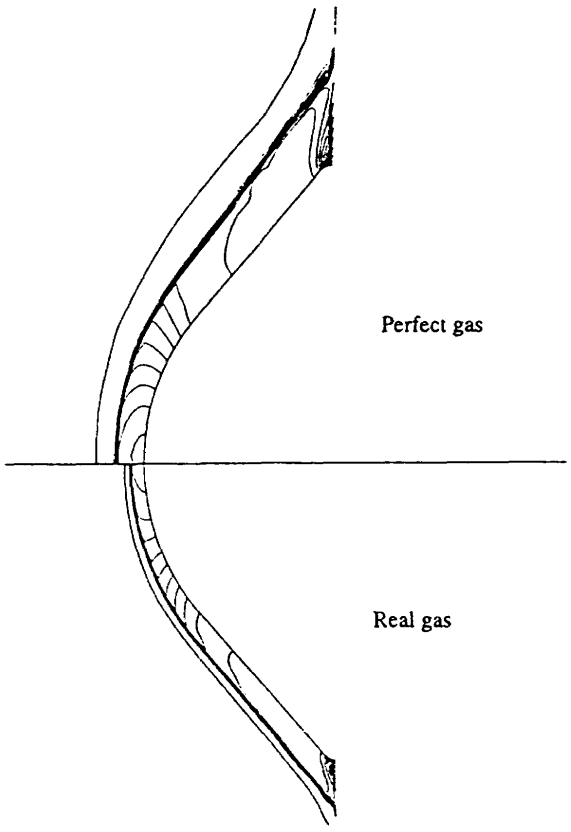

Fig. 4 Pressure Contour Plots

Figure 5 shows the comparison of computed temperature contour plots. Figure 6 shows pressure distributions along the body surface. The y/r=0 point is the stagnation point. The pressure distribution of the real gas case is similar to that of the perfect gas case. Figure 7 shows temperature distribution along the stagnation line. The peak temperature of the perfect gas case is three times higher than that of the real gas case.

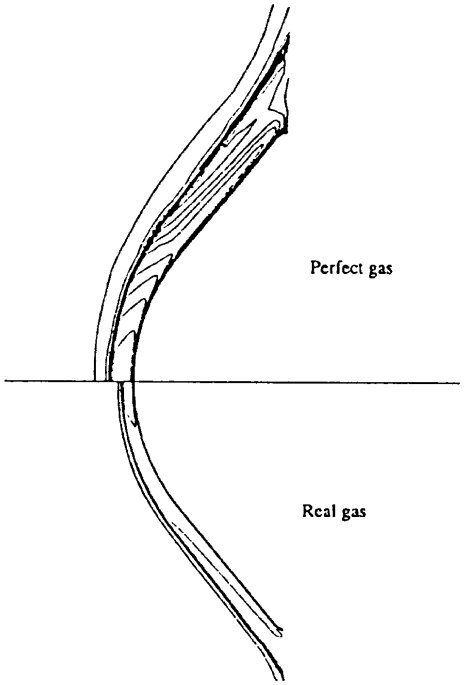

Fig. 5 Temperature contour plots

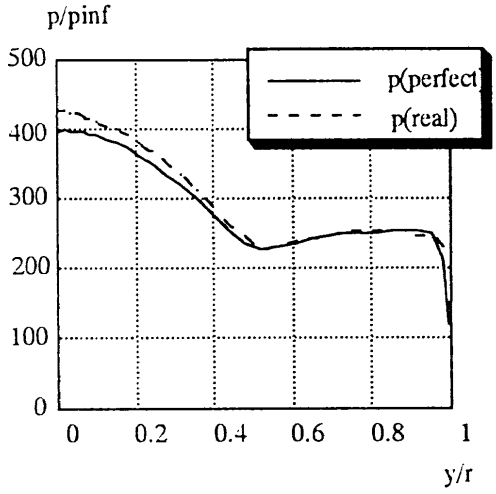

Fig. 6 Pressure Distribution along the body surface

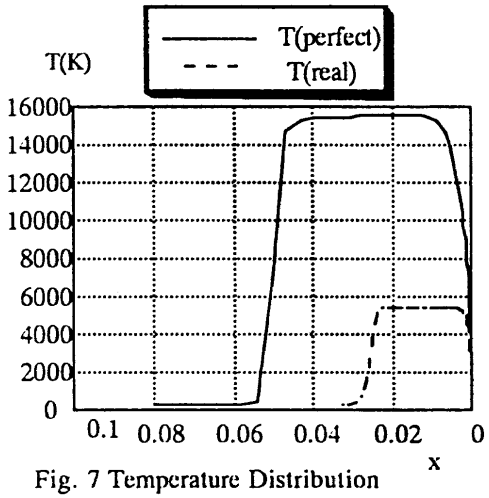

Fig. 7 Temperature Distribution along the stagnation line

Figure 8 shows the heat transfer distributions along the body surface. The maximum heat transfer of the perfect gas case is slightly higher than that of the real gas case.

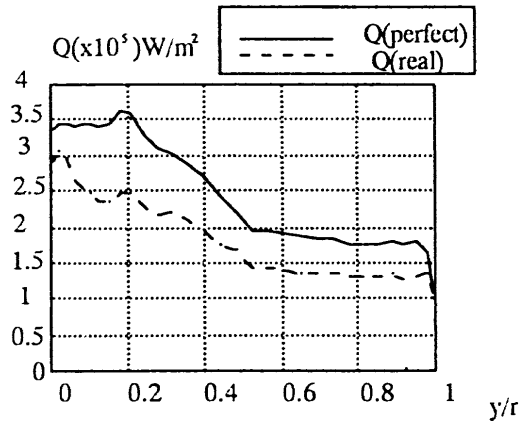

Fig.8 Heat Transfer Distribution along the body surface

The fluctuating characteristic near the stagnation point is thought to be caused by the artificial dissipation that added to cure the

carbuncle phenomena. The carbuncle phenomenon is one of the numerical instabilities in capturing a strong shock wave. The Roe scheme has this problem. The dissipative scheme, however, cannot catch the strong shock sharply and cannot simulate the heat transfer ratio accurately.

Figure 9 shows the air component distribution along the stagnation line. N2 and O2 are dissociated and NO and O appear in the region between the bow shock and the body. This dissociation absorbs the internal energy of the air.

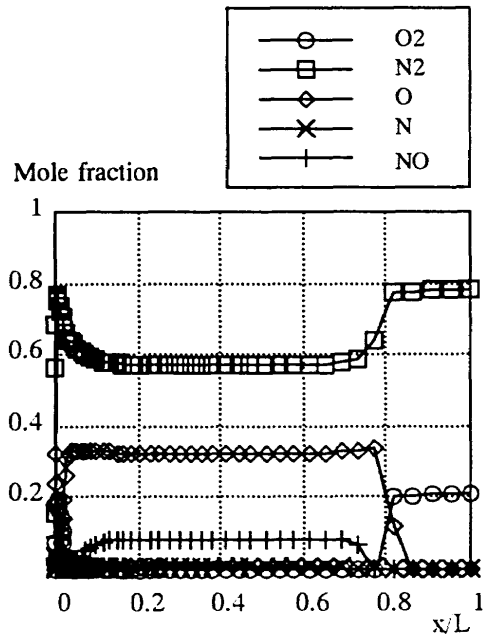

Fig.9 Chemical Component along the stagnation line

5. CONCLUSIONS

The flowfields around OREX is calculated by the MHI Navier-Stokes code(CHRIS). The real gas and perfect gas case are calculated. Results show the significant differences between the two cases in the shock stand-off distance and the temperature distribution. Some glitch due to the artificial dissipation is observed at the heat transfer distribution. The adaptation of a more robust and less dissipative scheme is now under the study.

REFERENCES

(1) Ota, D. K., Chakravarthy, S.R. and Darlin, J.C. , 'An Equilibrium Air Navier-Stokes Code for Hypersonic Flows," AIAA -88-0419.
(2) Prabhu, R.K., Stewart, J.R. and Thareja, R. R., 'A Navier-Stokes Solver for High Speed Equilibrium Flows and Application to Blunt Bodies,' AIAA-89-0668, 1989.
(3) Srinivasan, S., Tanehill, J.C. and Weilmuenster, K.J., 'Simplified Curve Fits for the Thermodynamic Properties of Equilibrium Air', NASA RP-1181, 1987.
(4) Roe, P. L., 'Characteristic-Based Schemes for the Euler Equations,' Fluid Mech. 1986. 18:337-365.
(5) Srinivasan, S., and Tanehill, J. C., 'Simplified Curve Fits for the Transport Properties of Equilibrium Air', NASA CR-178411, 1987.
(6)Fujii, K.,and Obayashi, S., 'High-Resolution Upwind Scheme for Vortical Flow Simulations,' Journal of Aircraft, Vol.226, No.12, December 1989, pp.1123-1129.
(7) Grossman, B. and Walters, R. W., 'An Analysis of Flux Split Algorithms for Euler Equations with Real Gases,' AIAA 87-1117.
(8) Prabhu, R.K., and Erickson, W. D., 'A Rapid Method for the Computation of Equilibrium Chemical Composition of Air of 15,000 K,' NASA TP-2797, 1988.